Fatigue Characteristics of a Glass-Fiber-Reinforced Polyamide

KOUICHI HANDA,[1] ATSUSHI KATO,[2] IKUO NARISAWA[3]

[1] Materials Research Laboratory, Nissan Research Center, Nissan Motor Co., Ltd., 1 Natsushima-cho, Yokosuka, Kanagawa 237, Japan

[2] Research Department, Nissan ARC, Ltd., 1 Natsushima-cho, Yokosuka, Kanagawa 237, Japan

[3] Materials Engineering Department, College of Engineering, Yamagata University, 4 Jonan, Yonezawa, Yamagata 992, Japan

Received 1 June 1998; accepted 14 September 1998

ABSTRACT: This paper deals with prediction of the temperature rise in the stress-controlled fatigue process of a glass-fiber-reinforced polyamide and the application of a temperature and frequency superposition procedure to the S-N curve. An experimental equation was derived to predict the temperature rise from calculations based on the fatigue test conditions and viscoelastic properties of the material. The temperature rise (ΔT) can be expressed as a product of a coefficient term $\Phi(L, \kappa)$ concerning heat radiation and the test-specimen shape and a function term P_{fat} concerning the viscoelastic properties and fatigue test conditions. $\Phi(L, \kappa)$ was found experimentally to derive the equation for predicting the temperature rise blow or above the glass transition temperature (T_g) of the material. The equation $\sigma_R = -S_{Tf} A \log N_{fR} + S_{Tf} B$ was obtained as a procedure for applying temperature and frequency superposition to S-N curves in consideration of ΔT. This procedure was obtained by combining both temperature- and frequency-superposition techniques. Here, σ_R and $\log N_{fR}$ represents the stress and the fatigue lifetime calculated at a given temperature and frequency, A and B denote the slope and intercept of any arbitrarily chosen S-N curve, and S_{Tf} is a shift factor for temperature and frequency superposition. © 1999 John Wiley & Sons, Inc. J Appl Polym Sci 72: 1783–1793, 1999

Key words: fatigue; glass-fiber-reinforced polyamide; prediction of the temperature rise; temperature and frequency superposition procedure

INTRODUCTION

Polymer composite materials have been increasingly applied in recent years to structural components requiring higher levels of strength, like metal substitutes, in order to achieve weight and cost reductions. One important strength criterion that must be met in applying composite materials to structural components is fatigue life.[1] From the standpoint of structural component design, it is essential to be able to predict fatigue life accurately and quickly. However, predicting the fatigue life of resins reliably has traditionally been an enormously time-consuming task because of the lack of suitable accelerated-testing procedures that could be applied to polymer composite materials. In an effort to overcome this problem, Jinen,[2] Furuhashi et al.,[3] and Karger–Kocsis[4] proposed resin fatigue mechanisms that took into account material failure. Somiya et al.[5] also re-

Correspondence to: K. Handa.

Journal of Applied Polymer Science, Vol. 72, 1783–1793 (1999)

ported an attempt to apply Miner's law to fatigue-life predictions of resin materials. Those studies, however, did not result in a procedure that would allow the fatigue life of resin materials to be predicted uniformly and quickly under various types of conditions.

It is well known that heat generation originating from viscoelasticity occurs during the fatigue process of resin materials. Shults[6] suggested that a portion of the deformation energy accompanying cyclic stressing of test pieces contributes to heat generation. Kajiyama et al.[7–10] pointed out that understanding the heat generation process of test pieces is an important factor in predicting the fatigue life of resin materials. This temperature rise is closely related to the surrounding temperature because the viscoelastic loss itself is a function of temperature and changes rapidly in the vicinity of the glass transition temperature. There are several early studies[11–13] that have dealt with the influence of specimen temperature on the fatigue behavior of polymers. The mechanisms of fatigue fracture below and above glass transition temperature were analyzed in terms of stress-activated kinetic theories. However, because the kinetic theories are based on the molecular failure mechanisms such as main-chain scissions or second-bond ruptures, these early results cannot be directly applied to the fiber-reinforced polymers, which are macroscopically inhomogenous.

The purpose of this study is to examine the relationship between the temperature rise observed during the fatigue life of a glass fiber-reinforced polyamide and that during fatigue test conditions. An attempt was made to apply a temperature and frequency superposition procedure to the S-N curves to predict the fatigue life from an engineering viewpoint.

This research examined the relationship between the temperature rise observed during the fatigue process of a glass fiber-reinforced polyamide and the fatigue test conditions. An attempt was made to apply a temperature and frequency superposition procedure to the S-N curves of the test polyamide.

EXPERIMENTAL

Test Material

Test specimens were injection molded from polyamide 66 containing 33% glass-fiber reinforcement (made by Asahi Chemical Industries, Tokyo, Japan, under the brand name of Leona 1042G). Figure 1 shows the shape and dimensions of an ASTM-D Type S tension-impact specimen. The moisture content of the specimens before and after the fatigue tests was kept to less than 0.2% by weight.

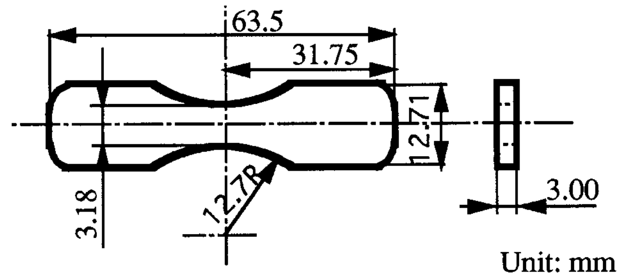

Figure 1 Dimensions of ASTM-D1822 Type S Tension-Impact Specimen.

Test Procedure

Stress-controlled fatigue tests were conducted using an electrohydraulic servo fatigue tester to apply cyclic tensile stress at frequencies from 5 Hz to 50 Hz over a temperature range from 273 K to 393 K. The minimum load applied was 49 N (minimum stress ≒ 0) and the maximum stress was in a range of 49–137 MPa. The surface temperature in the center of a specimen was continuously measured during the fatigue test with an infrared thermometer, producing a beam diameter of less than 3 mm, and CA thermocouples of less than 0.3 mm in diameter. The viscoelastic properties of the test material that were used in the calculations were measured with a DMTA MKII dynamic-stress rheometer (Polymer Laboratories Co., Ltd.). Measurements were made in a nitrogen atmosphere at a frequency of 20 Hz in a temperature range from 123 K to 523 K and with a rate of temperature increase of 2°/min.

RESULTS AND DISCUSSION

S-N Curve Characteristics

Figure 2 shows the ambient temperature (T) dependence of the S-N curve of the polyamide 66 specimen at a frequency (f) of 20 Hz. The S-N curve can be approximated as a straight line in terms of the maximum stress (σ) and semilogarithmic plots of fatigue life ($\log N$). This indicates

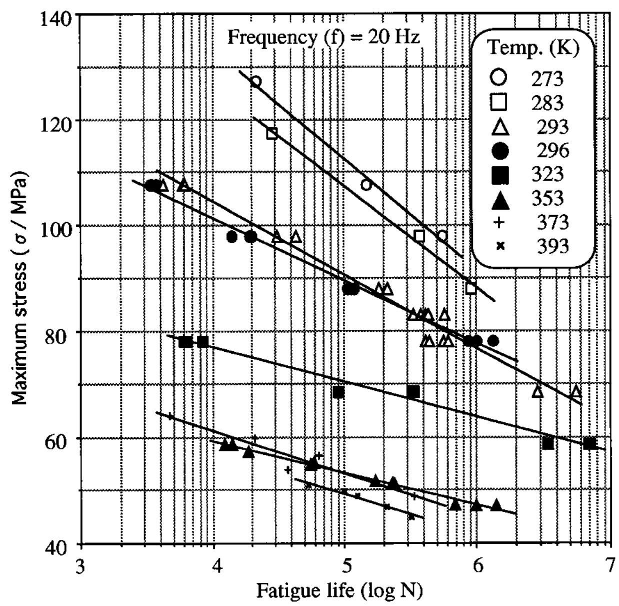

Figure 2 Dependence of S-N Curve on Ambient Temperature.

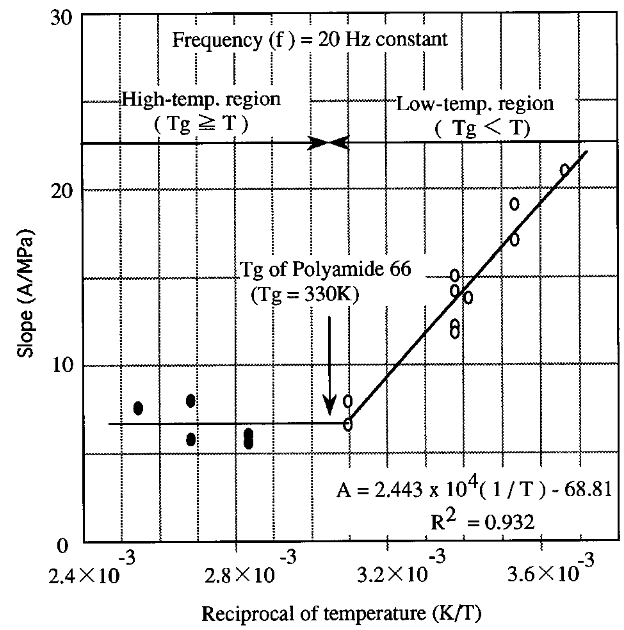

Figure 3 Relationship Between Ambient Temperature (T) and Slope (A) of S-N Curve.

that the S-N curve can be approximated with the following general equation:

$$\sigma = -A \log N + B \tag{1}$$

where A and B are the slope and intercept of the approximated S-N curve, respectively. The temperature dependence of the slope A and intercept B of the approximated S-N curve is shown in Figures 3 and 4. Both the slope and the intercept show a good linear correlation with the reciprocal of the ambient temperature ($1/T$). This relationship tends to divide into two regions at the glass transition temperature (T_g = 330 K) of polyamide 66. In the low-temperature region below the glass transition temperature, both the slope and the intercept tended to decrease with increasing temperature. In the high-temperature region above the glass transition temperature, the slope and the intercept did not display any noticeable temperature dependence and it is inferred that both had nearly constant values. These results suggest, then, that the fatigue mechanism of the test specimens differed depending on whether their temperature exceeded the glass transition temperature or not.

The frequency dependence of the S-N curve at 300 K is shown in Figure 5. In this figure as well, the S-N curve can be approximated as a straight line in terms of the maximum stress (σ) and semi-logarithmic plots of fatigue life (log N) and can be approximated with eq. (1). The frequency dependence of the slope A and intercept B is shown in Figures 6 and 7. Both figures indicate that the slope and intercept decreased linearly with increasing frequency. These results suggest that

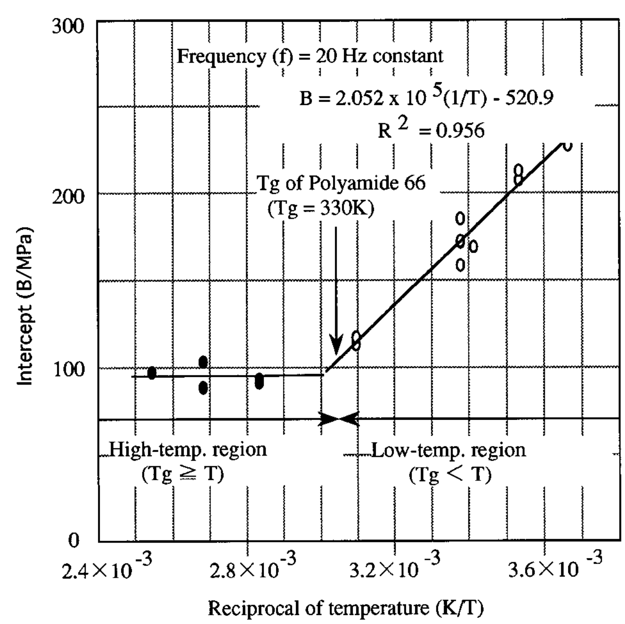

Figure 4 Relationship Between Temperature (T) and Intercept (B) of S-N Curve.

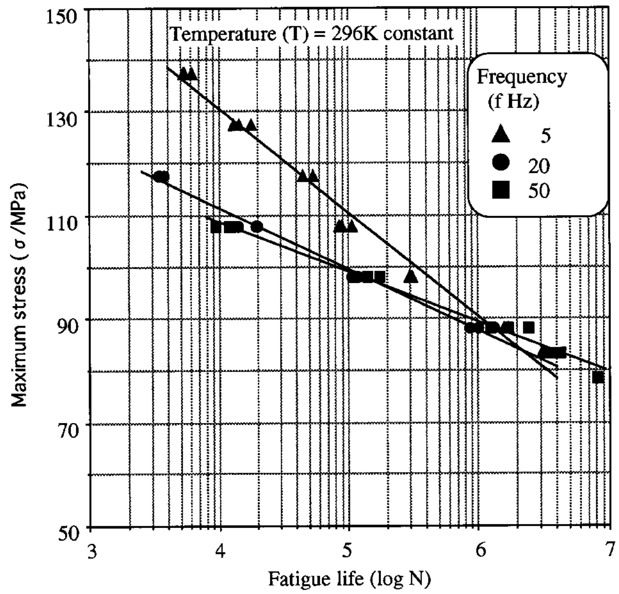

Figure 5 Dependence of S-N Curve on Cyclic Frequency (f).

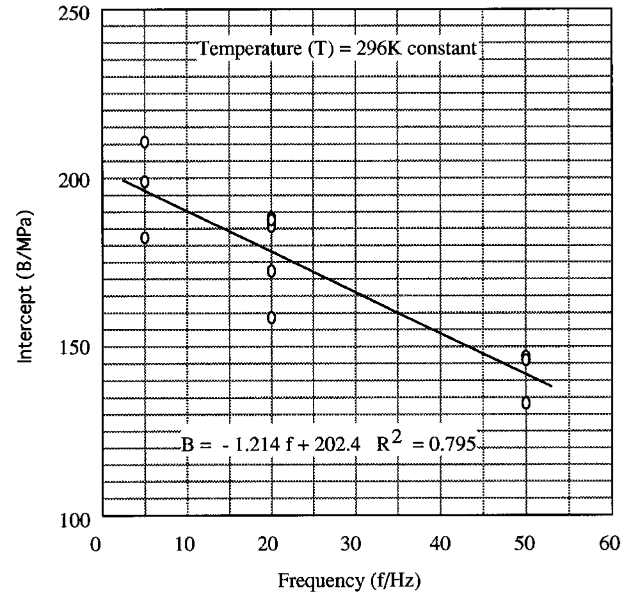

Figure 7 Relationship between Cyclic Frequency (f) and Intercept (B) of S-N Curve.

fatigue developed according to the same mechanism at all of the frequencies measured in these fatigue tests.

Heat Generation Behavior and Method of Predicting Temperature Rise

Temperature Rise at Specimen Surface Accompanying Fatigue

Figure 8 shows the difference (ΔT) between the surface temperature of the test specimen (T_s) and the ambient temperature (T_o) as a function of the number of fatigue cycles (N). The specimen surface temperature shows a sharp rise in a short period of time in the initial and final fatigue stages of the test. Throughout the middle fatigue stage, which accounted for most of the fatigue life, the specimen surface temperature shows little change, indicating a quasi-thermal equilibrium state. The structural changes associated with fatigue appear to have proceeded gradually during the middle stage, which represented the major

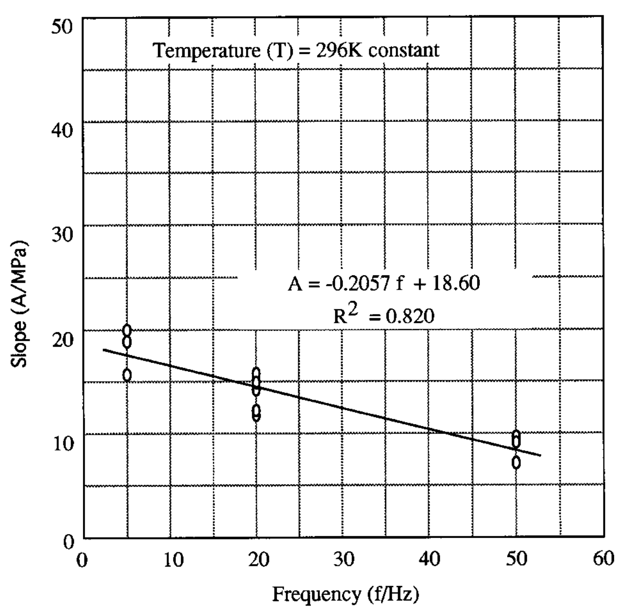

Figure 6 Relationship Between Cyclic Frequency (f) and Slope (A) of S-N Curve.

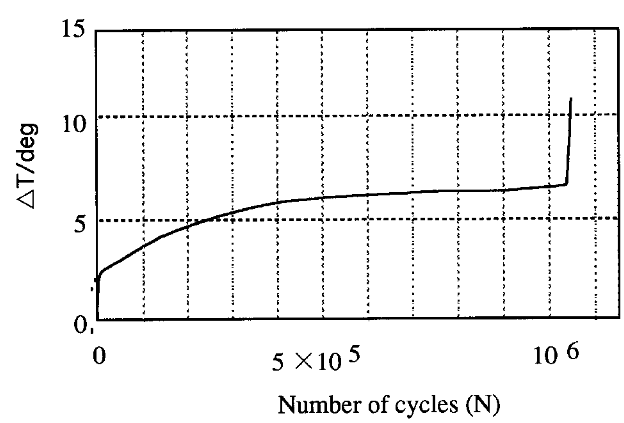

Figure 8 Relationship between temperature rise (ΔT) and number of cycles (N) during fatigue tests at ambient temperature of 296 K, maximum stress of 88 MPa and frequency of 20 Hz.

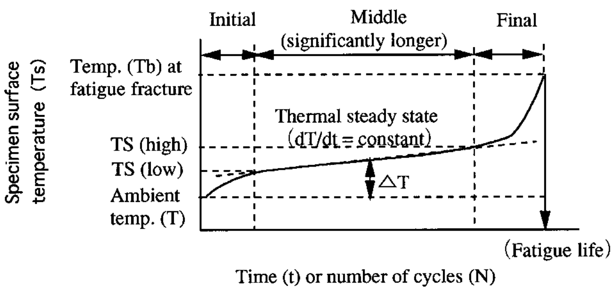

Figure 9 Definition of temperature rise (ΔT) at specimen surface.

portion of fatigue life. It is thought, therefore, that the temperature rise at the specimen surface during the middle fatigue stage has a large influence on fatigue life.

The middle fatigue stage was regarded as a quasi-thermal equilibrium state and the temperature rise (ΔT) was defined as indicated in Figure 9 and eq. (2). An attempt was then made to predict the temperature rise.

$$\Delta T = \{(T_{S(\mathrm{High})} + T_{S(\mathrm{Low})})/2\} - T_o \qquad (2)$$

where $T_{S(\mathrm{High})}$ and $T_{S(\mathrm{Low})}$ indicate the upper and lower limits of the specimen surface temperature in the middle fatigue stage.

Expression for Predicting Temperature Rise

The following discussion concerning the heat balance in the middle fatigue stage is based on the equation proposed by Kajiyama et al.[7–10] Based on research conducted with polyethylene (PE) fibers and other materials, Kajiyama and Takahara[7] reported that the hysteresis loss H_T per unit time and unit volume in pulsating strain-controlled fatigue can be expressed as a function of the square of the average strain ε_{av}, as represented by the following equation:

$$H_T = \pi f E''_{\mathrm{nl}} \varepsilon_{\mathrm{av}}^2 \qquad (3)$$

where f is the frequency and E''_{nl} is the nonlinear loss modulus.

In the present work, the term E''_{nl} = E″, denoting the loss modulus in linear viscoelasticity, was applied to allow simple viscoelastic treatment, and eq. (3) was rewritten as eq. (4) below.

$$H_T = \pi f E'' \varepsilon_{\mathrm{av}}^2 \qquad (4)$$

where E'' is the linear loss modulus.

A stress-controlled fatigue test was then conducted under a virtually pulsating stress condition (minimum stress $\sigma_{\min} \fallingdotseq 0$, maximum stress, or hysteresis stress $\sigma_{\max} \gg 0$). The dynamic modulus of elasticity E' during the fatigue test was expressed by eq. (5) based on the frequency response and taking into account the viscoelastic properties of the tested resin.

$$E' = \Sigma E_i(\omega^2\tau_i^2)/(1 + \omega^2\tau_i^2) \qquad (5)$$

where E_i is the modulus of elasticity of the i^{th} viscous element, ω is the angular frequency and τ_i is the relaxation time of the i^{th} viscous element.

The relationship expressed by eq. (5) can be simplified to

$$E' = E(\omega^2\tau_i^2)/(1 + \omega^2\tau_i^2) \qquad (6)$$

where E is the static modulus of elasticity.

Because resin are viscoelastic bodies, the relationship $0 < \tau < \infty$ holds true. Additionally, under the fatigue conditions used in this study, 5 Hz $\leqq \omega/2\pi \leqq$ 50 Hz. Because it is possible to assume that $1 \ll \omega^2 \tau^2$, eq. (6) can be approximated as eq. (7).

$$E' \fallingdotseq E \qquad (7)$$

It is well known that the frequency at which resin fatigue accompanying fatigue heat generation can be observed is higher than several Hz. Accordingly, the relationship express by eq. (7) is thought to be valid.

Assuming that there is a linear viscoelastic relationship between strain ε and stress σ in strain-controlled fatigue, the following expression is obtained:

$$\varepsilon_{\mathrm{av}} = \varepsilon_{\max}/2 = (\sigma_{\max}/2)/E \qquad (8)$$

where $\varepsilon_{\max}$ is the maximum strain and $\sigma_{\max}$ is the maximum stress.

Equation (9) was therefore derived from eqs. (4) and (8).

$$H_T = \pi f E''\{(\sigma_{\max}/2)/E'\}^2 \qquad (9)$$

Viscoelastic energy loss H_T is consumed as the energy dissipated in structural changes and as heat generation. On the basis of the viscoelastic properties in Figure 10 and the photomicrographs of the test pieces in Figure 11, it is concluded that

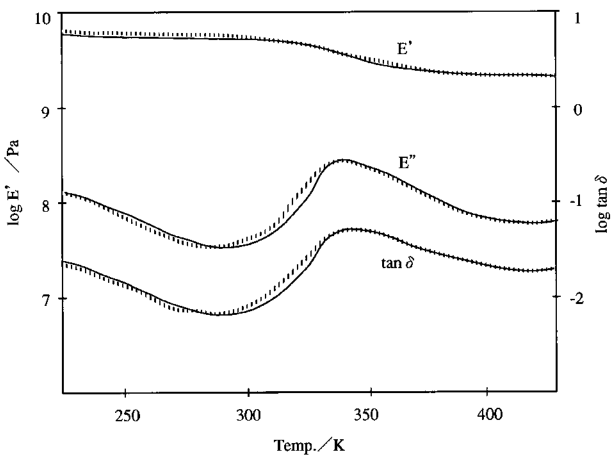

Figure 10 Dependence of viscoelastic behavior on cycle number during fatigue process — after 10^4 cycle · · · · · after 10^6 cycle.

there was little change in energy loss associated with structural changes in the initial and final periods of the middle fatigue stage. It is thought therefore that nearly all of H_T was consumed as heat generation in the middle fatigue stage. Then, assuming that all of the energy of H_T is converted to heat, and also by transforming eq. (9), the amount of heat released Q_F can be given by:

$$Q_F = \pi f(E''/E'^2)(\sigma/2)^2 \tag{10}$$

where E' is the storage modulus of elasticity and σ is the maximum stress ($\sigma_{\max}$).

The amount of heat radiated Q_R into the ambient environment from the surface area S in a given unit of time can be found from the following expression:

$$Q_R = (S/V)\kappa\Delta T = \kappa\Delta T/L \tag{11}$$

where S is the surface area of the specimen, V is the volume of the specimen, κ is the heat transfer coefficient, and L is the length of the specimen. Accordingly, from eqs. (10) and (11), the change in the surface temperature of the specimen per unit of time, dT/dt, due to heat generation and radiation can be given by:

$$\begin{aligned} dT/dt &= (Q_F - Q_R)/\rho C_P \\ &= [\pi f(E''/E'^2)(\sigma/2)^2 - \kappa\Delta T/L]/\rho C_P \quad (12) \end{aligned}$$

where ρ is the density and C_P is the specific heat of the specimen, respectively.

Moreover, because the middle fatigue stage is a quasi-thermal equilibrium state, it is assumed that $dT/dt = 0$. Then, eq. (12) can be expressed by eqs. (13) and (14):

$$0 = [\pi f(E''/E'^2)(\sigma/2)^2 - \kappa\Delta T/L]/\rho CP \tag{13}$$

$$\Delta T = (\pi L/\kappa)f(E''/E'^2)(\sigma/2)^2 = \Phi(L, \kappa)P_{\text{fat}} \tag{14}$$

where

$$\Phi(L, \kappa) = \pi L/\kappa \tag{15}$$

$$P_{\text{fat}} = f(E''/E'^2)(\sigma/2)^2 \tag{16}$$

This indicates that the temperature rise ΔT is the product of the coefficient term $\Phi(L, \kappa)$ concerning the heat release and the test specimen shape, and of the function term P_{fat} concerning the viscoelastic properties of the test specimen and the fatigue test conditions. Accordingly, using eq. (14), $\Phi(L,$

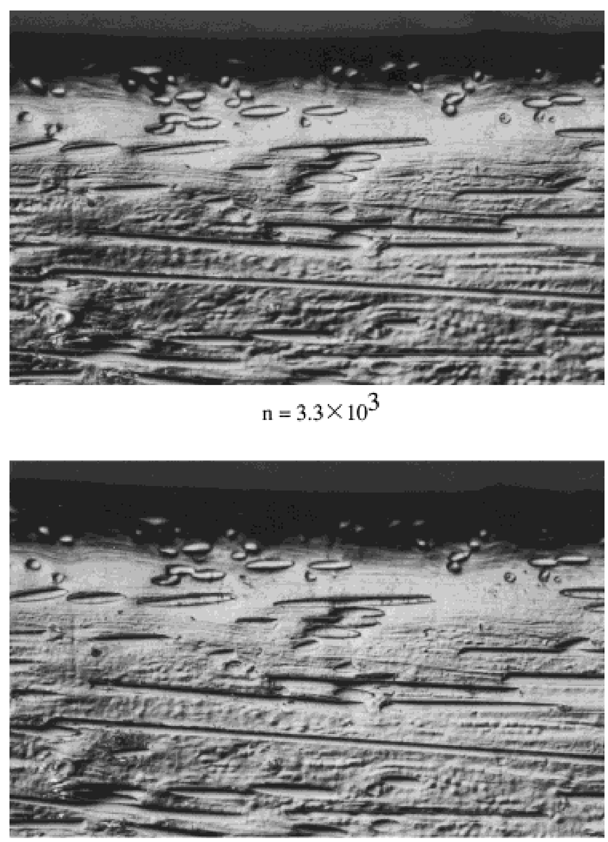

n = 3.3× 10^3

n = 1.1× 10^6

Figure 11 Photomicrographs of specimens during fatigue process.

κ) can be determined experimentally because ΔT is simply proportional to P_{fat}.

Method of Calculating Temperature Rise

Figure 12 shows the temperature rise (ΔT) as a function of P_{fat} for the various temperatures used in the fatigue tests, and Figure 13 shows the same relationship for the different frequencies used. The two figures indicate that there was nearly a proportional relationship between (ΔT) and P_{fat}, as predicted by eq. (13). The slope of this approximate equation is $\Phi(L, \kappa)$.

The curves for the relationship between (ΔT) and P_{fat} under the various test temperatures indicate that the slope tended to increase with increasing temperature. Discontinues are also seen in the slope of these ΔT vs. P_{fat} curves in the vicinity of the glass transition temperature (330 K) of polyamide 66. These discontinuities are thought to be attributable to large changes that occurred in the heat-transfer coefficient and viscoelastic properties at around that temperature.

The curves for the relationship between ΔT and P_{fat} under the different frequencies used in the fatigue tests indicate, on the other hand, that the slope tended to decrease with increasing frequency. Two reasons can be considered for this tendency. One is that the heat-transfer coefficient increased at higher frequencies (i.e., the apparent heat-transfer coefficient increased because of higher air velocity along the surface of the test specimen). The other is that the viscoelastic energy contribution to ΔT decreased (i.e., the contribution to structural change increased).

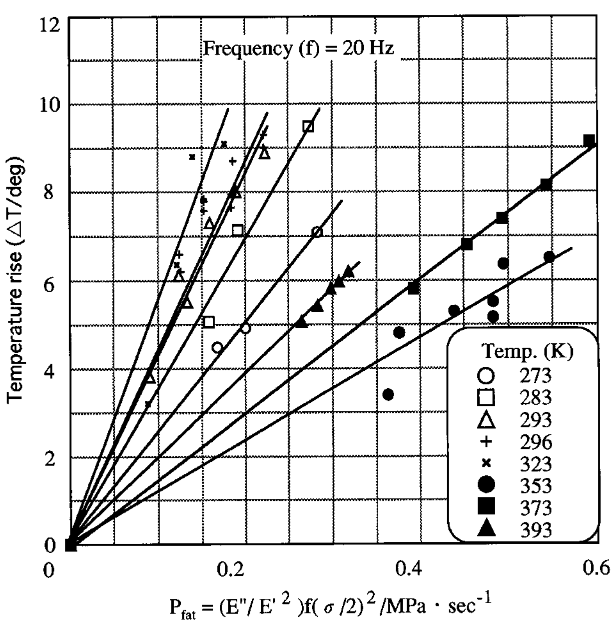

Figure 12 Effect of ambient temperature (T) on the parameter (P_{fat}) vs. temperature rise (ΔT) during fatigue tests.

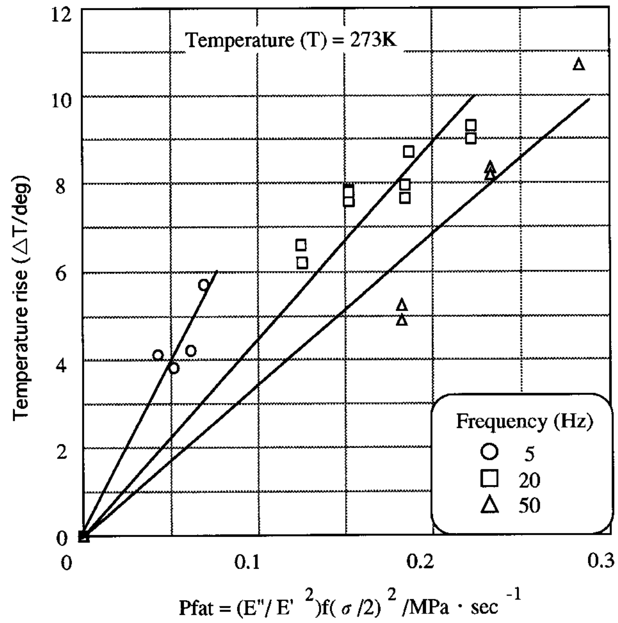

Figure 13 Effect of cyclic frequency (f) on the parameter (P_{fat}) vs. temperature rise (ΔT) during fatigue tests.

A study was then made of a method for calculating the coefficient ($\pi L/\kappa$) of eq. (14) from the ambient temperature and the frequency. Figure 14 shows the temperature and frequency (T/f) dependence of this coefficient ($\pi L/\kappa$). It is seen from the figure that a good linear correlation was obtained with each variable. Moreover, as noted earlier, the correlation with the ambient temperature divides into two approximated straight lines in the vicinity of the glass transition temperature (330 K) of polyamide 66. The results in Figure 14 thus indicate that temperature dependence in the region below the glass transition temperature can be expressed experimentally by eq. (17), and frequency dependence by eq. (18).

$$(\pi L/\kappa) = 10.72\ (T/f) - 116.7 \tag{17}$$

$$(\pi L/\kappa) = 0.8163\ (T/f) + 32.16 \tag{18}$$

Similarly, temperature dependence in the region above the glass transition temperature can be expressed experimentally by eq. (19), and frequency dependence by eq. (20).

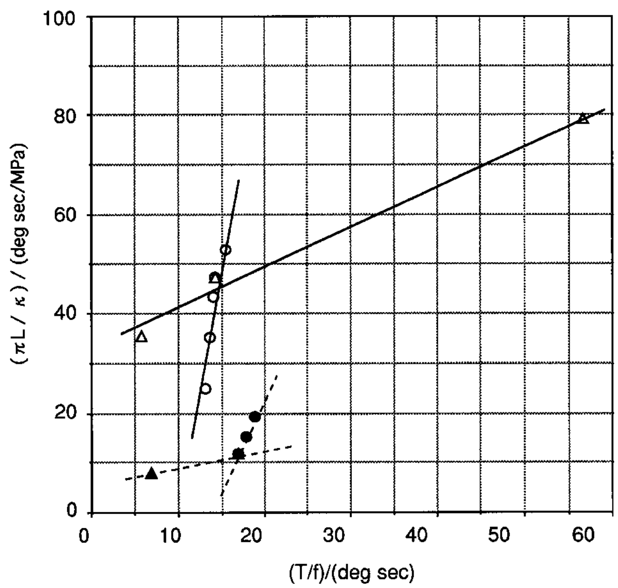

Figure 14 Relationship between the variables (T/f) and $(\pi L/\kappa)$ Low-temperature region ($T_g \geqq T$) ○ Dependence on T △ Dependence on f High-temperature region ($T_g < T$) ● Dependence on T ▲ Dependence on f.

$$(\pi L/\kappa) = 3.800\ (T/f) - 55.40 \tag{19}$$

$$(\pi L/\kappa) = 0.3721\ (T/f) + 5.233 \tag{20}$$

The foregoing procedure has shown that the coefficient $(\pi L/\kappa)$ in eq. (14) can be calculated from the fatigue test conditions (ambient temperature and frequency), and that the temperature rise ΔT can be found from the relationship between the calculated result and P_{fat}. Although not shown here, a comparison of the calculated and experimental results revealed that they were in good agreement.

Temperature/Frequency Superposition Method for S-N Curves

By analogy with the theory of viscoelasticity, it is thought that temperature and frequency superposition can be applied to S-N curves in order to take into account the fatigue test conditions under the same fatigue mechanism. The procedure used here for temperature and frequency superposition allows temperature superposition and frequency superposition to be applied alternately to any arbitrarily chosen S-N curves. The following discussion presents the results obtained when this temperature- and frequency-superposition procedure was applied to S-N curves in the low-temperature region below the glass transition temperature of polyamide 66.

Temperature Superposition Procedure

The S-N curves at ambient temperatures T_1 and T_2 are expressed by Eqs. (21) and (22):

$$\sigma_1 = -A_1 = \log N_1 + B_1 \tag{21}$$

$$\sigma_2 = -A_2 \log N_2 + B_2 \tag{22}$$

In the case of temperature superposition, the slopes A of the curves given by eqs. (21) and (22) must be equal. To accomplish this, a shift factor S_T is introduced to correct the slope of the curve given by eq. (22), and the expression is rewritten as eq. (23):

$$S_T \sigma_2 = -S_T A_2 \log N_2 + S_T B_2 \tag{23}$$

where S_T is defined as $S_T = A_1/A_2$.

In order for eq. (23) to be superposed on eq. (21), $S_T\sigma_2$ must equal σ_1.

$$-A_1 \log N_1 + B_1 = -S_T A_2 \log N_2 + S_T B_2 \log N_1 - \log N_2 = (B_1/A_1) - (B_2/A_2) \tag{24}$$

where the fatigue life shift factor S_{TN} is defined as indicated in eq. (25).

$$S_{TN} = (B_1/A_1) - (B_2/A_2) \tag{25}$$

Hence, the general equation for temperature superposition can be expressed as:

$$\sigma_{TR} = -S_T A(\log N + S_{TN}) + S_T B = -S_T A \log N_{TR} + S_T B \tag{26}$$

where σ_{TR} represents the stress calculated at a given temperature and $\log N_{TR}$ represents fatigue life calculated at that temperature and is expressed as $\log N_{TR} = \log N + S_{TN}$.

Figure 15 shows that the S-N curves in Figure 2 can be superposed on a standard S-N curve (20 Hz, 296 K) by using eq. (26). It should be noted that S_T and S_{TN} are dependent on $\Delta T(f, T)$.

Frequency Superposition Procedure

Although frequency superposition can also be accomplished in the same manner as for temperature, the simple superposition of the number of

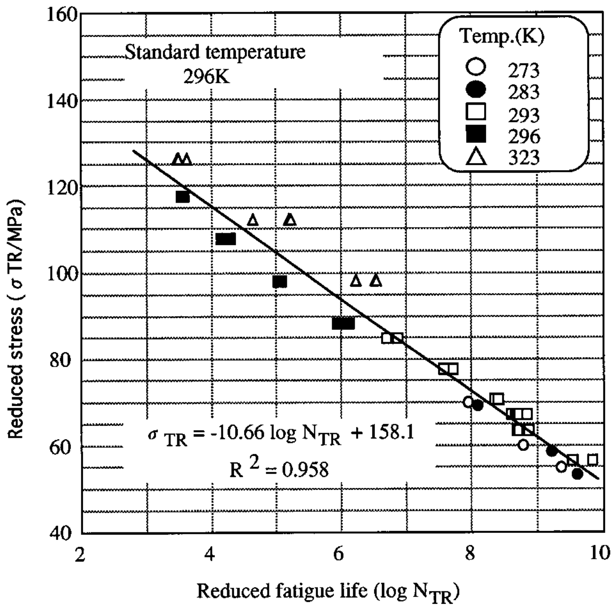

Figure 15 Temperature Superposition of S-N Curve.

cycles to fatigue failure N would result in different fatigue life figures owing to the frequency differences. Therefore, it is necessary to perform the following correction. The S-N curves are first expressed by eqs. (21) and (22) similar to the procedure for temperature, and the life time differences are then corrected according to the frequency differences.

The relationship between the number of cycles to fatigue failure N and the frequency f and fatigue life t at the frequencies f_1 and f_2 can be expressed by eqs. (27) and (28), respectively.

$$N_1/f_1 = t_1 \tag{27}$$

$$N_2/f_2 = t_2 \tag{28}$$

Equations (27) and (28) are introduced here to rearrange the basic S-N curve expressions, eqs. (21) and (22), in terms of fatigue life, resulting in eqs. (29) and (30):

$$\sigma_1 = -A_1 \log(N_1/f_1) + B_1 \tag{29}$$

$$\sigma_2 = -A_2 \log(N_2/f_2) + B_2 \tag{30}$$

Just as in the case of temperature superposition, frequency superposition requires that the slopes A of the curves given by eqs. (29) and (30) be equal. To achieve that equality, the shift factor S_f is introduced to correct the slope of the curve given by eq. (30), and the expression is rewritten as

$$S_f\, \sigma_2 = -S_f A_2 \log(N_2/f_2) + B_2 \tag{31}$$

where S_f is defined as $S_f = A_1/A_2$.

In order for eq. (31) to be superposed on eq. (29), $S_f\sigma_2$ must equal σ_1.

$$\begin{aligned} -A_1 \log(N_1/f_1) + B_1 &= -S_T A_2 \log(N_2/f_2) \\ &\quad + S_T B_2 \log N_1 - \log N_2 = (B_1/A_1) \\ &\quad - (B_2/A_2) + \log(f_2/f_1) \end{aligned} \tag{32}$$

where the fatigue life shift factor S_{fN} at the frequency of interest is defined as indicated in eq. (33).

$$S_{fN} = (B_1/A_1) - (B_2/A_2) + \log(f_2/f_1) \tag{33}$$

where log (f_2/f_1) is the term for correcting fatigue life differences due to frequency differences. Hence, the general equation for frequency superposition can be expressed as:

$$\begin{aligned} \sigma_{fR} &= S_f A(\log N + S_{fN}) + S_f B \\ &= -S_f A \log N_{fR} + S_f B \end{aligned} \tag{34}$$

where σ_{fR} represents the stress calculated at a given frequency and log N_{fR} denotes the fatigue life calculated at that frequency and is expressed as log N_{fR} = log $N + S_{fN}$.

Figure 16 indicates that the S-N curves in Figure 5 can be superposed on a standard S-N curve (20 Hz, 296 K) by using eq. (34). It should be noted that S_f and S_{fN} are dependent on $\Delta T(f, T)$.

Temperature and Frequency Superposition Procedure

As shown in Figure 17, two approaches can be considered for accomplishing the superposition of both temperature and frequency in which the temperature superposition procedure and the frequency superposition procedure are applied alternately. Assuming that the procedure is not dependent on the order of superposition, it can be expressed by eq. (35):

$$\begin{aligned} \sigma_R &= -S_T S_f A(\log N + S_{TN} + S_{fN}) + S_T S_f B \\ &= -S_{Tf} A(\log N + S_{TfN}) + S_{Tf} B \\ &= -S_{Tf} A \log N_{fR} + S_{Tf} B \end{aligned} \tag{35}$$

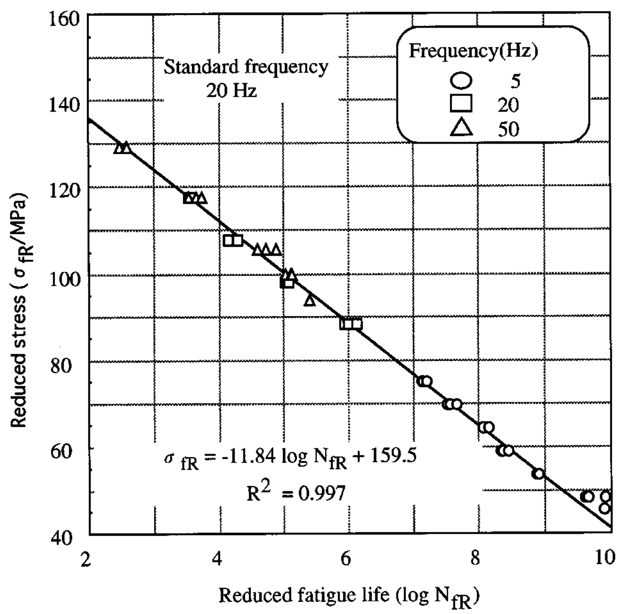

Figure 16 Frequency Superposition of S-N Curve.

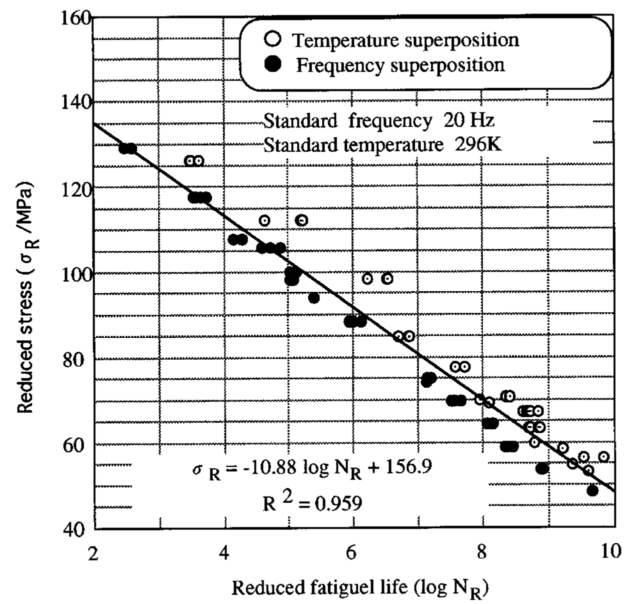

Figure 18 Universal S-N Curve in Low Temperature Region ($T \leqq T_g$).

where σ_R represents the stress calculated at a given temperature and frequency, A and B are the slope and the intercept of any arbitrarily selected S-N curve, and log N_{fR} denotes the fatigue life calculated at the given temperature and frequency and is expressed by eq. (36):

$$\log N_{fR} = \log N + S_{TfN} \tag{36}$$

where S_{Tf} and S_{TfN} are shift factors for temperature and frequency superposition and are given by eqs. (37) and (38), respectively:

$$S_{Tf} = S_T S_f \tag{37}$$

$$S_{TfN} = S_{TN} + S_{fN} \tag{38}$$

It should be noted that their values are dependent on $\Delta T(f, T)$.

Figure 18 shows that the S-N curves in Figures 2 and 5 can be superpositioned on a standard S-N curve (20 Hz, 296 K) by using eq. (35).

The foregoing discussion has shown that the temperature and frequency superposition procedure can be applied to the S-N curves of glass fiber reinforced polyamide 66.

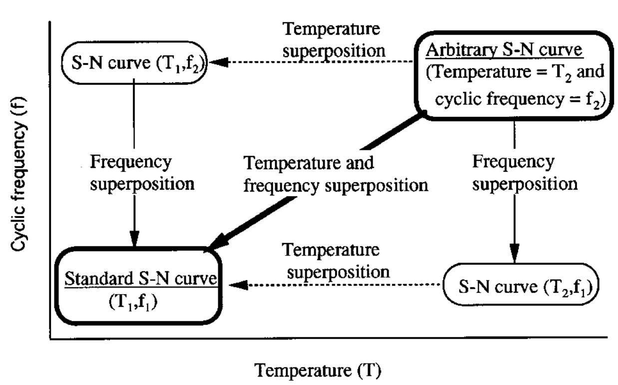

Figure 17 Procedure for Temperature- and Frequency-Superposition.

CONCLUSIONS

Trying to predict the temperature rise that occurs in the fatigue process of polymer composite materials and the associated S-N curves by experimentation is a time-consuming task. This research examined a method of predicting the temperature rise for a glass-fiber-reinforced polyamide and the possible application of a temperature and frequency superposition procedure to its S-N curve.

The temperature rise (ΔT) can be expressed as a product of a coefficient term $\Phi(L, \kappa)$ concerning heat radiation and the test specimen shape and a function term P_{fat} concerning the viscoelastic properties and fatigue test conditions. The coefficient term $\Phi(L, \kappa)$ was found experimentally to derive the equation for predicting the temperature rise. One equation is used in the low-temperature region below the glass transition temperature (T_g) of the material and a separate equation in the high-temperature region above that point. The values calculated for each temperature region showed good agreement with the experimental data.

The equation $\sigma_R = -S_{Tf}A \log N_{fR} + S_{Tf}B$ was obtained as a procedure for applying temperature and frequency superposition to S-N curves in consideration of ΔT. This procedure was obtained by combining both temperature and frequency superposition techniques.

It was shown that the use of the proposed methods allows the temperature rise of a test specimen at any arbitrarily chosen ambient temperature and frequency, as well as its S-N curve, to be predicted quickly from the measured viscoelastic properties of the material and the fatigue test conditions. As a result, it is expected that the practical application of these methods will lead to a substantial reduction in development lead time for applying polymer composite materials to structural components with high-strength requirements.

This paper has presented some of the results obtained in research conducted by the Study Group on Resin Fatigue, which consists of members from Yamagata University, Asahi Chemical Industry Co., Ltd., Ube Industries, Ltd., DuPont Corp., Toray Industries, Inc., Polyplastics Co., Ltd., Mitsui Petrochemical Industries, Ltd., Mitsui Toatsu Chemicals, Inc. and Nissan Motor Co., Ltd. The authors thank the individuals at the companies concerned for their helpful discussions in connection with this research.

REFERENCES

1. Narisawa, I. Journal of the Society of Fiber Science and Technology, Japan 1985, 41, 81.
2. Jinen, E. Transactions of the Society of Polymer Science, Japan 1980, 33, 499.
3. Furuhashi, Y.; Hori, Y. Transactions of the Japan Society of Mechanical Engineers (A) 1980, 45, 423.
4. Karger-Kocsis, J. Composites 1990, 21, 243.
5. Somiya, S.; Ohta, M.; Kunio, T. Summaries of Lectures Given at the Annual Meeting of the Japan Society of Mechanical Engineers 1985, 66, 45.
6. Shults, J. M. Treat Mater Sci Technol 1977, 10, 599.
7. Kajiyama, T.; Takahara, A. Journal of the Japan Rubber Industries Association 1986, 59, 34.
8. Kajiyama, T.; Takahara, A. Journal of the Society of Fiber Science and Technology, Japan 1990, 46, 413.
9. Takahara, A.; Yamada, K.; Kajiyama, T. J Appl Polym Sci 1985, 26, 1085.
10. Kajiyama, T. New Materials 1993, 1, 50.
11. Regel, V. R.; Leksovskij, A. M. Inten J Fract Mech 1967, 2, 99.
12. Regel, V. R.; Leksovskij, A. M. Mecha, Polimerov 1969, 1, 70.
13. Zilvar, V. J Macromol Sci-Phys 1971, B5, 273.